

Letter to the Editor



Projections of Temperature-related Non-accidental Mortality in Nanjing, China*

SUN Qing Hua¹, Radley M. Horton², Daniel A. Bader², Bryan Jones³,
ZHOU Lian⁴, and LI Tian Tian^{1,#}

The health effects of climatic changes constitute an important research area, yet few researchers have reported city- or region-specific projections of temperature-related deaths based on assumptions about mitigation and adaptation. Herein, we provide quantitative projections for the number of additional deaths expected in the future, owing to the cold and heat in the city of Nanjing, China, based on 31 global circulation models (GCMs), two representative concentration pathways (RCPs) (RCP4.5 and RCP8.5), and three population scenarios [a constant scenario and two shared socioeconomic pathways (SSPs) (SSP2 and SSP5)], for the periods of 2010-2039, 2040-2069, and 2070-2099. The results show that for the period 2070-2099, the net number of temperature-related deaths can be comparable in the cases of RCP4.5/SSP2 and RCP8.5/SSP5 owing to the offsetting effects attributed to the increase of heat related deaths and the decrease of cold-related deaths. In consideration of this adaptation, we suggest that RCP4.5/SSP2 is a better future development pathway/scenario.

Key words: Heat effect; Cold effect; Mortality projection; Representative concentration pathways/ Shared socioeconomic pathways

The global average temperature trends have indicated a yearly temperature increase of 0.85 °C from 1880 to 2012^[1]. Accordingly, the positive shift of temperature throughout the world is unequivocal. The World Health Organization (WHO) estimates that approximately 250,000 additional deaths will occur every year as a result of the anticipated climatic change within the period 2030-2050^[2]. In view of the seriousness of this issue, it is important to focus on human health projections given the

expected climatic changes, with the aim of implementing informed policy making decisions.

We selected Nanjing in China as a case study city. This study analyzed cold- and heat-related mortality relationships from existing historical data, and projected cold- and heat-related deaths using 31 global circulation models (GCMs) and two representative concentration pathways (RCPs; RCP4.5 and RCP8.5) radiative forcing scenarios to estimate future temperatures. It also estimated the future population number based on three population scenarios, including a constant scenario and two shared socioeconomic pathways (SSPs) (SSP2 and SSP5).

The estimation of future deaths associated with climatic changes consisted of two stages: (1) the estimation of the temperature-mortality relationship between the historic daily mortality and the daily temperatures of Nanjing by taking into account the air pollutants, and the (2) assessment of future death risks with the a) use of the temperature-mortality relationship from stage 1 and b) the projection of future temperatures by taking into account the future population.

A Poisson regression model combined with a distributed lag linear and non-linear models (DLNM) was used to assess the relationship between temperature and daily deaths. All historic (2007-2012) data were obtained from the Jiangsu Provincial Center for Disease Control and Prevention. The health effect parameters comprise the daily numbers of all internal causes of death of urban Nanjing residents (ICD-10 codes A00-R99). Meteorological data, including the daily mean temperature and daily mean relative humidity, were

doi: 10.3967/bes2019.019

*National Natural Science Foundation of China [Grant: 91543111]; Beijing Natural Science Foundation [7172145]; Special Foundation of Basic Science and Technology Resources Survey of Ministry of Science and Technology of China [No. 2017FY101204]; and National High-level Talents Special Support Plan of China for Young Talents.

1. National Institute of Environmental Health, Chinese Center for Disease Control and Prevention, Beijing 100021, China; 2. Center for Climate Systems Research, Columbia University, New York 10025, USA; 3. City University of New York Institute for Demographic Research, New York 10010, USA; 4. Jiangsu Provincial Center for Disease Control and Prevention, Nanjing 21009, Jiangsu, China

obtained from the Nanjing station in China (World Meteorological Organization, identification number: 58,238). Air pollution data, and data including daily PM₁₀ concentrations, daily SO₂ concentrations, and daily NO₂ concentrations, were obtained from the National Air Pollution Monitoring stations of Nanjing.

A general liner model (GLM) was used to estimate the association between daily mean temperature and mortality. We used a DLNM with a natural cubic spline with five degrees-of-freedom for temperature, and a natural cubic spline with three internal knots placed at equally spaced values with a lag up to 14 days. The covariates were adjusted accordingly. Specifically, a natural cubic spline with seven degrees-of-freedom per year was used to account for the season and long-term trends, and a natural cubic spline with three degrees-of-freedom was used to account for the daily mean relative humidity, daily mean concentrations of PM₁₀, NO₂, and SO₂, and the day of the week.

To determine the threshold of the temperature, we calculated the overall cumulative exposure-response association. A minimum mortality risk temperature (MMT) of 24.9 °C was determined and used as the reference temperature to calculate relative risks.

To check the robustness of the main model, we adjusted the potential modifications related to the modeling choices, exposure metrics, and air pollution. Sensitivity analyses of the exposure-response relationship investigated potential modifications related to model parameters and air pollution. All statistical analyses were performed using the software R (version 3.2.0).

We estimated future temperatures (for the periods of 2010-2039, 2040-2069, and 2070-2099) with 31 GCMs (Supplementary Table S1 available in www.besjournal.com) and two RCPs (RCP4.5 and RCP8.5). The baseline period was that used for the period of 1970-1999. The spatial average of the Bias Correction Spatial Disaggregation (BCSD) land-based grid boxes corresponded to the latitude and longitude coordinates of Nanjing (latitude: 31°14'-32°37', and longitude: 118°22'-119°14'). The details of the analyses were described previously^[3]. The distribution of the future average daily mean temperature is listed in Supplementary Table S2 (available in www.besjournal.com). The mean temperatures of the periods 2010-2039, 2040-2069, and 2070-2099, according to the RCP4.5 scenario

were 16.6 °C, 17.6 °C, and 18.1 °C, respectively. The mean temperatures of the periods 2010-2039, 2040-2069, and 2070-2099, according to the RCP8.5 scenario were 16.7 ± 9.5 °C, 18.3 ± 9.5 °C, and 20.2 ± 9.6 °C, respectively.

We used the 1990 (5.02 × 10⁶) population data from the Nanjing statistical yearbook (1991) to estimate the population in the period 1970-1999^[4]. The constant scenario assumes that the total population will remain constant with respect to the corresponding levels in the period 1970-1999 (5.02 × 10⁶). The population projections were obtained using the National Center for Atmospheric Research- the City University of New York (NCAR-CUNY) spatial population downscaling methodology^[5], and are in agreement with the SSP2 and SSP5 scenarios (Supplementary Table S3 available in www.besjournal.com). We projected the population at a resolution of 1/8° and for a ten year time interval. Based on the SSP2 and SSP5 scenarios we defined a) the population in the 2010-2039 as the average population of the years 2010, 2020, and 2030, b) the population of the 2040-2069 as the average of the years 2040, 2050, and 2060, and c) the population of the 2070-2099 as the average of the years 2070, 2080, and 2090. The future population in different scenarios is shown in Supplementary Table S4 (available in www.besjournal.com).

Projected deaths were estimated using the modeled projected daily mean temperature and the modeled population. The deaths relative to MMT were calculated to identify the heat effect for all the days with daily mean temperatures higher than MMT. For all the days with daily mean temperatures lower than MMT, the additional number of deaths-compared to MMT-were calculated to define the cold effect. The summations of heat-related and cold-related deaths were calculated to define the net effect according to Equation 1.

$$\Delta\text{Deaths} = Y_0 \times \text{ERC} \times \text{POP} \quad (1)$$

Where ΔDeaths is the daily number of the additional number of temperature-related deaths, and Y_0 is the baseline daily mortality rate (per 100,000 people). The non-accidental mortality rate in 2010 was used as the baseline daily mortality rate, and was obtained from the Nanjing Statistical Yearbook (2011)^[6] and the Chinese Center for Disease Control and Prevention. We assumed that the mortality rate will remain constant in the future. ERC is the percentage change in mortality for a specified change in temperature derived from the calculated

relative risk at each temperature based on the model analysis of the observed data, as described previously. POP is the population calculated based on the three population scenarios described previously. We computed heat-related deaths, cold-related deaths, and the deaths attributed to net effects (temperature related deaths) for each day. We then calculated the yearly mean deaths for each time period. Additionally, we defined cold and hot days which corresponded to the 15th percentiles of temperature for both extreme temperature cases (P15 for extreme cold, P75 for extreme heat effect) to compare the number of deaths attributed to cold and heat.

Table 1 lists a summary of the statistics of the various variables. Data spanning a total of 2,137 days were included in the analyses. The mean, minimum, and maximum daily mean temperatures in Nanjing during the study period were 16.2 °C, -4.5 °C, and 34.5 °C, respectively. The mean, minimum, and maximum daily numbers of non-accidental deaths were 94, 46, and 155, respectively.

Supplementary Figure S1 (available in www.besjournal.com) shows the overall cumulative temperature-mortality curve derived using DLNM. The MMT was 24.9 °C. This curve suggests that both

cold and heat deviations from MMT were associated with additional deaths. The results of sensitivity analyses of health effects with different parameters and different air pollutants were stable (Supplementary Table S5 available in www.besjournal.com). Relative Risks (RRs) were not substantially affected in the sensitivity models that were adjusted for *df* and lag, or those that included PM₁₀, NO₂, and SO₂.

Figure 1 shows that the annual cold-related deaths in RCP4.5 and RCP8.5 will continue to decrease if we do not take into account the change of population (constant population scenario). In the cases of the SSP2 and SSP5 population scenarios, the annual cold-related deaths in RCP4.5 and RCP8.5 will increase in the 2010-2039, and then decrease after the 2040-2069. In general, the annual heat-related deaths in RCP4.5 and RCP8.5 will increase for all the three population scenarios. According to the results of the constant scenario, the additional number of cold-related deaths for RCP4.5 was higher than those for RCP8.5. This finding was consistent at lower temperatures. With respect to the heat effects, the opposite was true. In the case of the net effect, the additional number of death counts (median of the

Table 1. Mean, Range, and Specific Percentiles for Variables Measured on a Daily Basis

Items	N	\bar{x}	Minimum	25th	75th	Maximum
Mean temperature (°C)	2,137	16.2	-4.5	8.0	24.4	34.5
Mean relative humidity (%)	2,137	70.2	17.0	61.0	81.0	99.0
Death number attributed to all internal causes (ICD10: A00-R99)	2,137	94	46	82	105	155
PM ₁₀ concentration (µg/m ³)	2,135	102.9	6.0	65.0	128.5	563.0
SO ₂ concentration (µg/m ³)	2,137	0.04	0	0.02	0.05	0.19
NO ₂ concentration (µg/m ³)	2,137	0.05	0	0.04	0.06	0.16

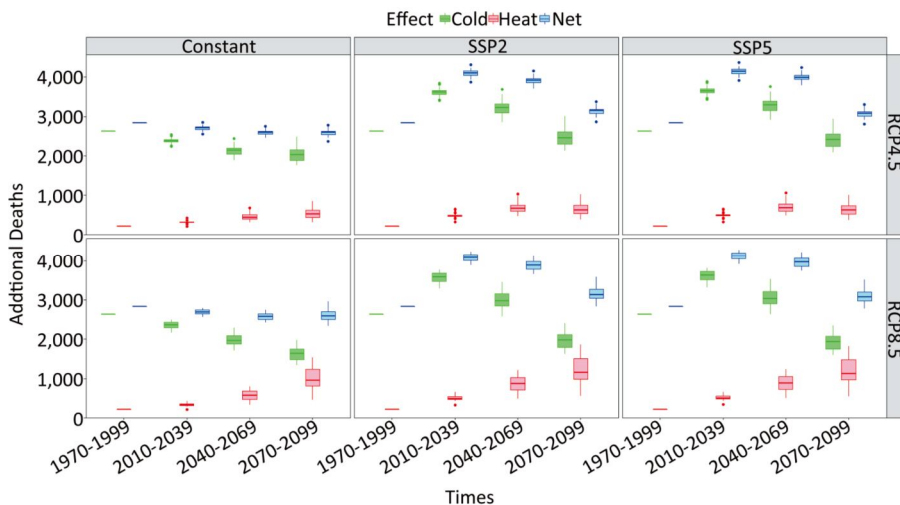


Figure 1. Projected cold, heat, and net temperature-related deaths from the period 1970-1999 to the 2070-2099 for RCP4.5 and RCP8.5 based on the three population scenarios and the 31 GCMs.

results obtained from the 31 GCMs) of RCP4.5 (2,705, 2,595, and 2,596) were higher for RCP8.5 (2,685, 2,570, and 2,584) in the 2010-2039, 2040-2069, and 2070-2099. The results related to the extreme cold and heat conditions listed in Supplementary Table S6 (available in www.besjournal.com).

To provide an overall perspective, we assessed the projected risk of the additional number of deaths

based on a set of SSP and RCP matrices (Supplementary Figure S2 available in www.besjournal.com), even though not all the combinations of RCPs and SSPs are internally consistent given the assumptions associated with the RCPs and SSPs (e.g., RCP8.5 and SSP1)^[7].

Figure 2 shows the median percentage change of cold, heat, and the net temperature-related deaths

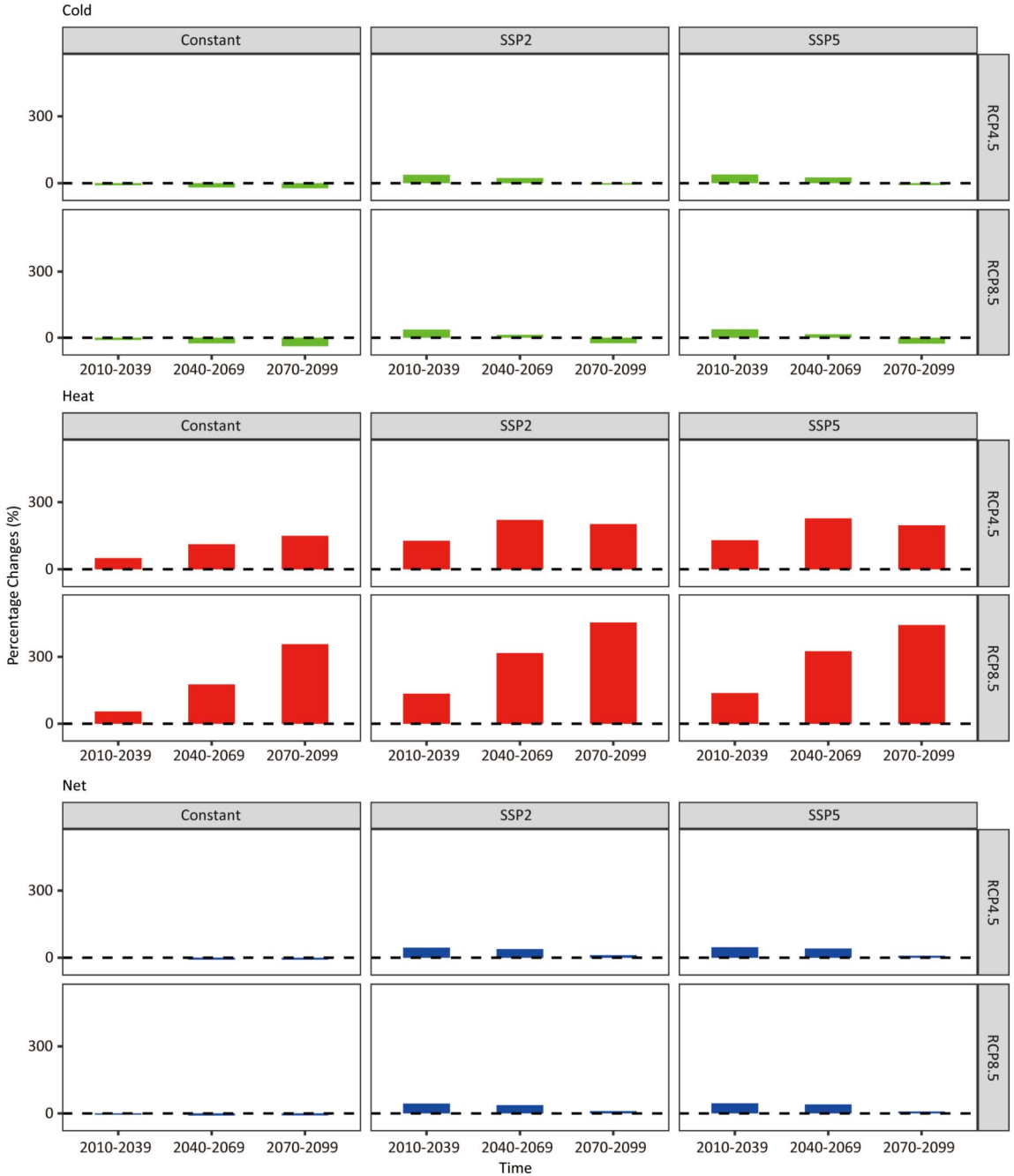


Figure 2. Percentage changes of medians of cold, heat, and net temperature-related deaths from the period 1970-1999 for RCP4.5 and RCP8.5 based on the three population scenarios.

in the 2010-2039, 2040-2069, and 2070-2099, using the RCP4.5 and RCP8.5 for the three population scenarios. Cold-related deaths for the constant population scenario continued to gradually decrease since the period 1970-1999. In the cases of the SSP2 and SSP5 scenarios, cold-related deaths increased slightly in the 2010-2039, and then gradually decreased. In the 2070-2099, cold-related deaths decreased by 26% compared to those in the period 1970-1999. The median estimate of cold-related mortality increased by approximately 38%, 23%, and -6%, respectively, in the case of the pathway/scenario of RCP4.5/SSP2, and increased by approximately 38%, 15%, and -26%, in the case of the pathway/scenario of RCP8.5/SSP5. Heat-related deaths exhibited the largest changes compared to the baseline period (1970-1999). Heat-related deaths using RCP8.5 increased dramatically compared to those estimated based on the RCP4.5 scenario. The median estimates of heat-related mortalities increased by approximately 127%, 221%, and 202%, respectively, in the case of the pathway/scenario of RCP4.5/SSP2, and increased by approximately 137%, 325%, and 443%, in the case of the scenario of RCP8.5/SSP5. Temperature-related deaths will change slightly in the 2010-2039, 2040-2069, and 2070-2099 (-5% to -9%). In the 2070-2099, the amplification in SSP2 is expected to be slightly higher than SSP5, and both will increase slightly (8% to 11%). To eliminate the effects of population size changes, we also calculated the fractions attributed to each time period (Supplementary Table S7 available in www.besjournal.com).

Future scenario assumptions constitute some of the most challenging and consequential aspects of climatic impact projections in the health sector, especially the assumption of future temperature and future population, and the internal connection of these assumptions. The combination of RCPs and SSPs defines several family macroscale scenarios and interplays between adaptation and mitigation^[7]. In the estimations of future temperatures, we chose two RCP scenarios, i.e., RCP8.5 and RCP4.5, their use is consistent with the conduct of many prior studies^[8]. RCPs were developed to describe different forcing levels of future climate changes. In the projection of population, some studies assumed that the population would remain constant^[9]. Some other studies projected the population in a specific developmental scenario^[4]. We performed comparisons by alternating the population scenarios, including the constant population scenario, SSP2, and SSP5, to measure the population changes. Given the

internal assumptions of RCPs and SSPs, we chose two SSP scenarios in this study, i.e., SSP2 and SSP5. RCP4.5 and SSP2 may be internally consistent and so are the RCP8.5 and SSP5.

Owing to the offsetting effects on heat and cold deaths, the net numbers of temperature-related deaths in the 2070-2099 are expected to be comparable in the cases of the RCP4.5/SSP2 and RCP8.5/SSP5 pathways/scenarios. However, the ratio of cold-related and heat-related mortalities for the two scenarios were different. The RCP8.5/SSP5 scenario shows an increase in the heat-related mortality and a decrease in the cold-related mortality by a large margin. Nevertheless, the change in the pathway/scenario of RCP4.5/SSP2 is relatively smooth. These results were similar to those obtained from a previous research study conducted in the Jiangsu Province^[10]. From the aspect of human adaptability, we suggest that RCP4.5/SSP2 is a better future development pathway/scenario.

There are some limitations associated with our study. Although the population will adapt to temperature changes to some extent, and the temperature-mortality relationship and MMT can in fact change over time, the extent of this adaptation is still uncertain in Nanjing. Thus, we decided not to account for a) the adaptation, and to b) take into consideration the assumption that the temperature-mortality relationship MMT will remain constant in the future. We also did not consider the future changes in meteorological factors and air pollution, or the possible correlations between these factors that may also affect the temperature-mortality relationship. In addition, according to UN data, the population in China will change in the future, but there is no specific data available for Nanjing. To avoid the introduction of larger deviations, we assumed that the overall population mortality rate in Nanjing will remain constant in the future. Thus, we did not consider the possible change of the demographic structure.

Author Contribution Statement SUN Qing Hua: performed the exposure-response relationship analyses, mortality projections, and wrote the manuscript. Radley M. Horton: performed the temperature projection analyses and edited the manuscript. Daniel A. Bader: performed the temperature projection analyses. Bryan Jones: performed the population projection analyses. ZHOU Lian: supplied the data of Nanjing. LI Tian Tian: designed the work and edited the manuscript.

[#]Correspondence should be addressed to LI Tian Tian, Research Fellow, Doctor, E-mail: litiyantian@nieh.chinacdc.cn, Tel: 86-10-50930213

Biographical note of the first author: SUN Qing Hua, female, born in 1984, master, Assistant Research fellow, majoring in environmental health.

Received: September 19, 2018;

Accepted: January 11, 2019

REFERENCES

1. IPCC, 2014: Climate Change 2014: Synthesis Report. Contribution of Working Groups I, II and III to the Fifth Assessment Report of the Intergovernmental Panel on Climate Change [Core Writing Team, R.K. Pachauri and L.A. Meyer (eds.)]. IPCC, Geneva, Switzerland, 151.
2. WHO, Quantitative risk assessment of the effects of climate change on selected causes of death, 2030s and 2050s. 2014; Switzerland.
3. Li TT, Horton RM, Bader DA, et al. Aging Will Amplify the Heat-related Mortality Risk under a Changing Climate: Projection for the Elderly in Beijing, China. *Sci Rep*, 2016; 20, 28161.
4. Bureau NS. Nanjing statistical yearbook (1991). http://221.226.86.104/file/nj2004/1991/renkouyulaodongli/3_2.htm. [2016-9-13] (In Chinese)
5. Jones B, O'Neill BC. Spatially explicit global population scenarios consistent with the Shared Socioeconomic Pathways. *Environ Res Lett*, 2016; 8, 084003.
6. Bureau NS. Nanjing statistical yearbook (2011). Available from: <http://221.226.86.104/file/nj2004/2011/renkou/3-1.htm>. [2016-9-13] (In Chinese)
7. van Vuuren DP, Kriegler E, O'Neill BC, et al. A new scenario framework for Climate Change Research: scenario matrix architecture. *Clim Change*, 2014; 3, 373-86.
8. Li T, Horton R, Bader D, et al. Long-term projections of temperature-related mortality risks for ischemic stroke, hemorrhagic stroke, and acute ischemic heart disease under changing climate in Beijing, China. *Environ Int*, 2018; 112, 1-9.
9. Li TT, Horton RM, Kinney PL. Projections of seasonal patterns in temperature-related deaths for Manhattan, New York. *Nat Clim Change*, 2013; 8, 717-21.
10. Chen K, Horton RM, Bader DA, et al. Impact of climate change on heat-related mortality in Jiangsu Province, China. *Environ Pollut*, 2017; 224, 317-25.

Supplementary Table S1. Global Climate Models Used in This Study

Climate Model Acronym	Institution	Atmospheric Resolution (latitude × longitude)
ACCESS1-0	CSIRO (Commonwealth Scientific and Industrial Research Organization, Australia), and BOM (Bureau of Meteorology, Australia)	1.25° × 1.875°
BCC-CSM1-1	Beijing Climate Center, China Meteorological Administration	2.8125° × 2.8125°
BCC-CSM1-1-M	Beijing Climate Center, China Meteorological Administration	T106
BNU-ESM	College of Global Change and Earth System Science, Beijing Normal University	2.8125° × 2.8125°
CanESM2	Canadian Centre for Climate Modelling and Analysis	1.875° × 1.875°
CCSM4	National Center for Atmospheric Research	0.9° × 1.25°
CESM1-BGC	National Science Foundation, Department of Energy, National Center for Atmospheric Research	0.9° × 1.25°
CESM1-CAM5	National Science Foundation, Department of Energy, National Center for Atmospheric Research	0.9° × 1.25°
CMCC-CM	Centro Euro-Mediterraneo per I Cambiamenti Climatici	0.75° × 0.75°
CNRM-CM5	Centre National de Recherches Meteorologiques/Centre European de Recherche et Formation Avances en Calcul Scientifique	2.8° × 2.8°
CSIRO-Mk3-6-0	Commonwealth Scientific and Industrial Research Organisation in collaboration with the Queensland Climate Change Centre of Excellence	1.875° × 1.875°
FGOALS-G2	LASG, Institute of Atmospheric Physics, Chinese Academy of Sciences; and CESS, Tsinghua University	2.8125° × 2.8125°
FIO-ESM	The First Institute of Oceanography, SOA, China	2.8125° × 2.8125°
GFDL-CM3	Geophysical Fluid Dynamics Laboratory	200 km × 200 km
GFDL-ESM2G	Geophysical Fluid Dynamics Laboratory	2° × 2.5°
GFDL-ESM2M	Geophysical Fluid Dynamics Laboratory	2° × 2.5°
GISS-E2-R	NASA Goddard Institute for Space Studies	2° × 2.5°
HadGEM2-AO	National Institute of Meteorological Research/Korea Meteorological Administration	1.25° × 1.875°
HadGEM2-CC	Met Office Hadley Centre (additional HadGEM2-ES realizations contributed by Instituto Nacional de Pesquisas Espaciais)	1.25° × 1.875°
HasGEM2-ES	Met Office Hadley Centre (additional HadGEM2-ES realizations contributed by Instituto Nacional de Pesquisas Espaciais)	1.25° × 1.875°
INMCM4	Institute for Numerical Mathematics	1.5° × 2°
IPSL-CM5A-LR	Institut Pierre-Simon Laplace	3.75° × 1.9°
IPSL-CM5A-MR	Institut Pierre-Simon Laplace	2.5° × 1.25°
IPSL-CM5B-LR	Institut Pierre-Simon Laplace	3.75° × 1.9°
MIRCO-ESM	Japan Agency for Marine-Earth Science and Technology, Atmosphere and Ocean Research Institute (The University of Tokyo), and National Institute for Environmental Studies	2.8125° × 2.8125°
MIROC-ESM-CHEM	Japan Agency for Marine-Earth Science and Technology, Atmosphere and Ocean Research Institute (The University of Tokyo), and National Institute for Environmental Studies	2.8125° × 2.8125°
MIROC5	Atmosphere and Ocean Research Institute (The University of Tokyo), National Institute for Environmental Studies, and Japan Agency for Marine-Earth Science and Technology	1.40625° × 1.40625°
MPI-ESM-LR	Max Planck Institute for Meteorology (MPI-M)	1.8° × 1.8°
MPI-ESM-MR	Max Planck Institute for Meteorology (MPI-M)	1.8° × 1.8°
MRI-CGCM3	Meteorological Research Institute	320 × 160
NorESM1-M	Norwegian Climate Centre	1.9° × 2.5°

Supplementary Table S2. Distribution of Future Simulated Average Daily Mean Temperatures (°C) of 31 Models ($N = 517,116$)

	RCP4.5	RCP8.5
2020s		
Minimum	-7.0 (-8.0 to 5.0) ^a	-6.9 (-8.0 to -6.0)
1%	-1.0 (-2.0 to 0)	-0.9 (-2.0-0)
25%	8.1 (7.0 to 9.0)	8.3 (8.0 to 9.0)
50%	17.3 (17.0 to 18.0)	17.5 (17.0 to 18.0)
75%	24.9 (24.0 to 25.0)	25.0 (24.0 to 26.0)
99%	32.4 (31.0 to 33.0)	32.5 (32.0 to 33.0)
Maximum	35.1 (34.0 to 38.0)	35.2 (34.0 to 36.0)
Mean	16.6 (15.9 to 17.1)	16.7 (16.2 to 17.5)
SD	9.5 (9.1 to 9.7)	9.5 (9.1 to 9.7)
2050s		
Minimum	to 6.0 (-8.0 to -3.0)	-5.5 (-7.0 to -4.0)
1%	-0.1 (-2.0 to 1.0)	0.5 (-1.0 to 2.0)
25%	9.1 (8.0 to 10.0)	9.7(8.0 to 11.0)
50%	18.3 (17.0 to -20.0)	19.1 (18.0 to 21.0)
75%	25.7 (25.0 to 27.0)	26.6 (25.0 to 28.0)
99%	33.5 (32.0 to 35.0)	34.4 (33.0 to 336.0)
Maximum	36.1 (35.0 to 40.0)	36.8 (35.0 to 38.0)
Mean	17.6 (16.4 to 18.9)	18.3 (17.1 to 19.6)
SD	9.5 (9.1 to 9.7)	9.5 (9.1 to 9.9)
2080s		
Minimum	-5.6 (-8.0 to -3.0)	-3.6 (-6.0 to -2.0)
1%	0.4 (-2.0 to 2.0)	2.4 (1.0 to 4.0)
25%	9.5 (7.0 to 11.0)	11.6 (10.0 to 13.0)
50%	18.7 (17.0 to 20.0)	20.8 (19.0 to 23.0)
75%	26.5 (25.0 to 28.0)	28.5 (26.0 to 30.0)
99%	34.1 (32.0 to 36.0)	36.3 (34.0 to 39.0)
Maximum	36.7 (35.0 to 41.0)	38.7 (36.0 to 41.0)
Mean	18.1 (16.3 to 19.4)	20.2 (18.1 to 22.0)
SD	9.5 (9.0 to 10.0)	9.6 (8.9 to 10.2)

Note. ^aThe first number is the average of the minimum for each model. And the parentheses show the lowest minimum in any model and the highest minimum in any model.

Supplementary Table S3. Shared Socioeconomic Pathways (SSPs) Used in this Study

Scenarios	Definition
SSP1	This scenario assumes a future that is moving toward a more sustainable path, with educational and health investments accelerating the demographic transition, leading to a relatively low world population. The emphasis is on strengthening human wellbeing.
SSP2	This is the middle-of-the-road scenario in which trends typical of recent decades continue, with some progress toward achieving development goals, reductions in resource and energy intensity, and slowly decreasing fossil fuel dependency. Development of low-income countries is uneven, with some countries making good progress, while others are left behind.
SSP3	The scenario portrays a world separated into regions characterized by extreme poverty, pockets of moderate wealth, and many countries struggling to maintain living standards for rapidly growing populations. The emphasis is on security at the expense of international development.
SSP4	This is a world of high inequalities both among and within countries. There is increasing stratification between a well-educated, internationally connected society and a poorly educated society that works in labor-intensive industries.
SSP5	Worldwide, conventional development oriented toward economic growth is viewed as the solution to social and economic problems. Rapid development leads to energy systems dominated by fossil fuels, resulting in high greenhouse gas emissions. The emphasis on market solutions and globalization implies high migration.

Supplementary Table S4. Population of Baseline and Six Scenarios

Scenarios	Time Period	Population
Baseline	1980s	5.02×10^6
	2020s	6.32×10^6
Constant ^a	2050s	6.32×10^6
	2080s	6.32×10^6
	2020s	7.70×10^6
	2050s	7.75×10^6
SSP1	2080s	5.96×10^6
	2020s	7.62×10^6
	2050s	7.58×10^6
SSP2	2080s	6.08×10^6
	2020s	7.54×10^6
	2050s	7.42×10^6
SSP3	2080s	6.43×10^6
	2020s	7.68×10^6
	2050s	7.49×10^6
SSP4	2080s	5.36×10^6
	2020s	7.69×10^6
	2050s	7.74×10^6
SSP5	2050s	7.74×10^6
	2080s	5.96×10^6

Note. ^a The scenario of population keeps constant since 2010.

Supplementary Table S5. Sensitivity Analysis of Exposure-response Relationship

Item	health Effect	
	Cold effect ^a	Heat effect ^b
main model	1.41 (95% CI: 1.27-1.57)	1.14(95%CI:1.07-1.22)
model parameter		
df of time: 4	1.40 (96% CI: 1.29-1.53)	1.15 (95% CI: 1.10-1.21)
df of time: 5	1.43 (95% CI: 1.31-1.56)	1.13 (95% CI: 1.07-1.19)
df of time: 6	1.41 (95% CI: 1.27-1.55)	1.12 (95% CI: 1.06-1.19)
df of time: 8	1.35 (95% CI: 1.21-1.51)	1.13 (95% CI: 1.06-1.20)
df of time: 9	1.36 (95% CI: 1.20-1.54)	1.13 (95% CI: 1.05-1.22)
df of time: 10	1.39 (95% CI: 1.22-1.58)	1.14 (95% CI: 1.06-1.21)
lag period: 7	1.20 (95% CI: 1.11-1.30)	1.16 (95% CI: 1.10-1.22)
lag period: 10	1.33 (95% CI: 1.22-1.46)	1.14 (95% CI: 1.07-1.20)
lag period: 21	1.65 (95% CI: 1.45-1.88)	1.12 (95% CI: 1.03-1.22)
df of argvar: 3	1.37 (95% CI: 1.24-1.52)	1.09 (95% CI: 1.03-1.16)
df of argvar: 4	1.41 (95% CI: 1.27-1.57)	1.13 (95% CI: 1.05-1.20)
df of argvar: 6	1.40 (95% CI: 1.26-1.55)	1.14 (95% CI: 1.06-1.22)
df of argvar: 7	1.32 (95% CI: 1.18-1.48)	1.15 (95% CI: 1.07-1.23)
df of lk: 2	1.44 (95% CI: 1.29-1.59)	1.13 (95% CI: 1.06-1.20)
df of lk: 4	1.41 (95% CI: 1.27-1.57)	1.14 (95% CI: 1.07-1.22)
air pollution		
without air pollution	1.42 (95% CI: 1.28-1.57)	1.13 (95% CI: 1.06-1.21)
with PM ₁₀	1.42 (95% CI: 1.28-1.58)	1.13 (95% CI: 1.06-1.21)
with NO ₂	1.41 (95% CI: 1.28-1.57)	1.14 (95% CI: 1.06-1.21)
with SO ₂	1.41 (95% CI: 1.27-1.57)	1.14 (95% CI: 1.06-1.21)

Note. ^aThe change of mortality risk comparing the 99th percentile of the temperature distribution to MMT;

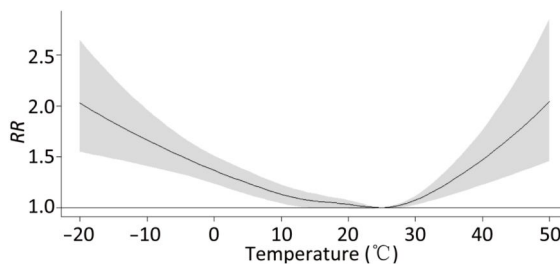
^bThe change of mortality risk comparing the 1st percentile of the temperature distribution to MMT.

Supplementary Table S6. Projection of Extreme Cold and Extreme Heat Related Deaths in the 2020s, 2050s, and 2080s for Different Population Scenarios and RCPs (median of 31GCMs)

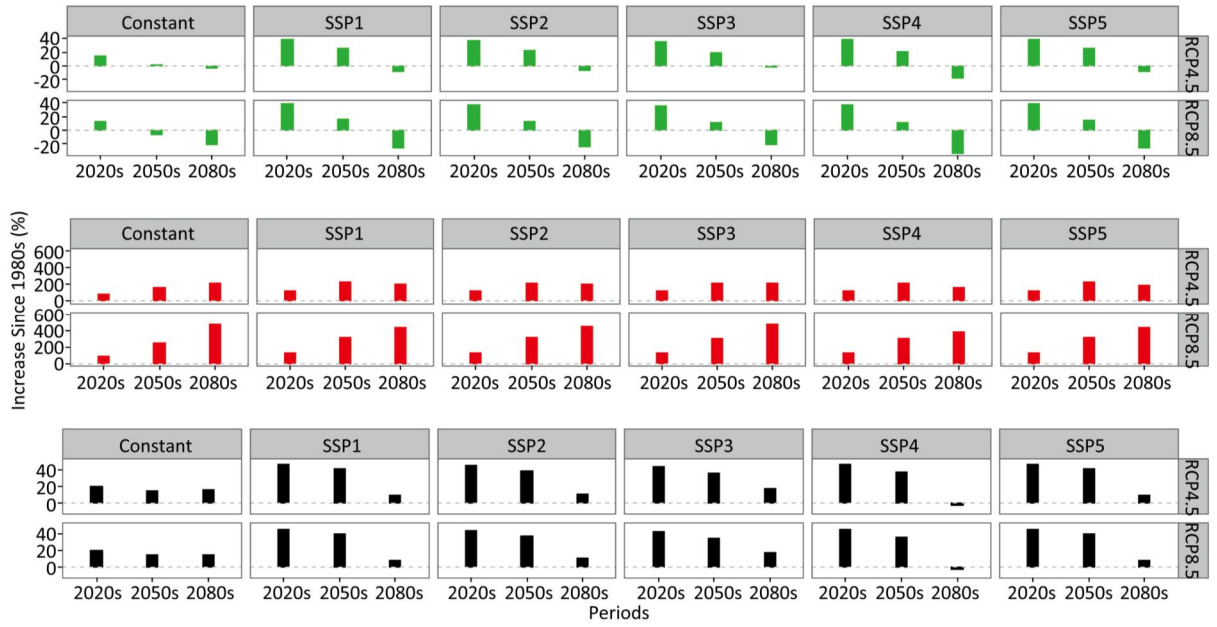
	RCP4.5/SSP2		RCP8.5/SSP5	
	Extreme Cold	Extreme Heat	Extreme Cold	ExtremeHeat
2020s	1421	466	1436	486
2050s	1016	659	721	875
2080s	678	622	262	1120

Supplementary Table S7. Attributable Fractions of Projected Cold, Heat, and Net Temperature-Related Death

			Cold	Heat	Net
1980s	RCP4.5	Constant	5.23×10^{-4}	4.13×10^{-5}	5.65×10^{-4}
		SSP2	5.23×10^{-4}	4.13×10^{-5}	5.65×10^{-4}
		SSP5	5.23×10^{-4}	4.13×10^{-5}	5.65×10^{-4}
	RCP8.5	Constant	5.23×10^{-4}	4.13×10^{-5}	5.65×10^{-4}
		SSP2	5.23×10^{-4}	4.13×10^{-5}	5.65×10^{-4}
		SSP5	5.23×10^{-4}	4.13×10^{-5}	5.65×10^{-4}
2020s	RCP4.5	Constant	3.77×10^{-4}	4.91×10^{-5}	4.28×10^{-4}
		SSP2	4.75×10^{-4}	6.19×10^{-5}	5.39×10^{-4}
		SSP5	4.75×10^{-4}	6.19×10^{-5}	5.39×10^{-4}
	RCP8.5	Constant	3.73×10^{-4}	5.07×10^{-5}	4.25×10^{-4}
		SSP2	4.70×10^{-4}	6.39×10^{-5}	5.35×10^{-4}
		SSP5	4.70×10^{-4}	6.39×10^{-5}	5.35×10^{-4}
2050s	RCP4.5	Constant	3.38×10^{-4}	6.96×10^{-5}	4.10×10^{-4}
		SSP2	4.26×10^{-4}	8.77×10^{-5}	5.17×10^{-4}
		SSP5	4.26×10^{-4}	8.77×10^{-5}	5.17×10^{-4}
	RCP8.5	Constant	3.10×10^{-4}	9.04×10^{-5}	4.06×10^{-4}
		SSP2	3.91×10^{-4}	1.14×10^{-4}	5.12×10^{-4}
		SSP5	3.91×10^{-4}	1.14×10^{-4}	5.12×10^{-4}
2080s	RCP4.5	Constant	3.21×10^{-4}	8.18×10^{-5}	4.11×10^{-4}
		SSP2	4.05×10^{-4}	1.03×10^{-4}	5.17×10^{-4}
		SSP5	4.05×10^{-4}	1.03×10^{-4}	5.17×10^{-4}
	RCP8.5	Constant	2.57×10^{-4}	1.50×10^{-4}	4.09×10^{-4}
		SSP2	3.25×10^{-4}	1.89×10^{-4}	5.15×10^{-4}
		SSP5	3.25×10^{-4}	1.89×10^{-4}	5.15×10^{-4}



Supplementary Figure S1. Overall cumulative association of temperature-mortality curve.



Supplementary Figure S2. Projection of percentage increase of cold, heat, and temperature-related deaths since the 1980s in the 2020s, 2050s, and 2080s for different population scenarios and RCPs (median of 31GCMs).